CHEMICAL ENGINEERING TRANSACTIONS
VOL. 57, 2017
A publication of AIDIC
The Italian Association of Chemical Engineering
Online at www.aidic.it/cet
Guest Editors: Sauro Pierucci, Jiří Jaromír Klemeš, Laura Piazza, Serafim Bakalis

ISBN 978-88-95608- 48-8; **ISSN** 2283-9216

Rehydrating Food Powders and Avoiding Lumps: Effect of Powder Properties and Liquid Flow

Xin Yi Ong[a], Spencer E. Taylor [b], Marco Ramaioli*[a]

[a]Department of Chemical and Process Engineering, University of Surrey, United Kingdom GU2 7XH
[b]Department of Chemistry, University of Surrey, United Kingdom GU2 7XH
m.ramaioli@surrey.ac.uk

Poor dispersion of beverages from dehydrated powders is a defect that obstructs the development of novel dehydrated food powders. We investigate how the physico-chemical properties of the powder grains affect the dispersion process. We used insoluble and non-cohesive grains to form islands of powders at a static water surface. Liquid "wicking" can avoid the formation of lumps, lead to complete sinking of powder grains when the grain contact angle is below a critical value in the range 51°-77°. The effect of grain size on powder sinking, or on the depth of island formed, was experimentally studied to understand the impact of particle size enlargement on powder dispersion. The interplay of grain contact angle and size was also quantitatively demonstrated. We also report the conditions leading to the detachment of a powder island from the interface, forming a powder lump that is wet outside and dry inside. Importantly, introducing flow in the liquid by agitation does not necessarily improve the dispersion process.

1. Introduction

Dehydrating food into a powder is a common method to increase its stability and reduce waste. However, the reconstitution of the food by rehydration of the powder can lead to unsatisfactory products quality due to the formation of partially dry lumps, which is a common observation in industrial processes and in the household. It is common to decouple this process into four successive or simultaneous stages of wetting, capillarity, dispersion and dissolution (Forny et al. 2011). When dispersing dehydrated powders in water, the physico-chemical properties of the powder: contact angle (Dupas et al. 2014), density (Dupas et al. 2015) and particle size (Mitchell et al. 2015) condition the hydration process of the powder matrix and its subsequent dissolution by the breaking up of particle agglomerates and aggregates into smaller units.

Agitation speed and hydrodynamic flow are also known to affect the dispersability of powders (Dupas et al. 2017). Although much effort has been put into the design of vessels and the types of impeller in order to improve the performance of dispersing particles in liquids in mechanically stirred systems, the mechanism by which lumps of powdered materials disperse in a liquid is not completely understood (Gurupatham et al. 2012). One of the main hurdles to overcome in the stirred vessel is the draw-down of floating particles from the liquid surface, as particles may float due to their poor wettability (Özcan-Taşkin 2006).

The position at which a spherical grain floats is governed by its weight, the surface tension force and the buoyancy force simultaneously satisfying a contact angle condition (Vella et al. 2005). However, for the case of a pile of spheres, the situation become more complicated as the contact line is no longer circular and the meniscus loses its axisymmetry (Cooray et al. 2017). Several studies (Hamlett et al. 2011; Raux et al. 2013) investigated spontaneous wicking in a compact pile of grains and found that the critical contact angle, θ^*, below which wicking takes place is considerably lower than 90˚. The contact angle below which wicking or detachment of powder island from the interface is measured for different grain sizes. The effect of liquid flow in the vicinity of the point of impact of the grains and how agitation facilitates the formation of lump during the dispersion process are then discussed.

2. Experimental Section

Four different sizes of glass beads (density, ρ_s = 2500 kg/m^3) were used in this study with diameters, d_p: <0.106, 0.212-0.300, <0.50 and 0.75-1.00 mm. By following the protocol proposed by Hamlett et al. (2011), the beads were immersed in a 1 mol/L hydrochloric acid solution for 1 h and then rinsed with deionised (DI) water and dried for 4 h at 60 °C. The hydrophilic glass beads were then silanised by treatment with a 5% dichlorodimethylsilane solution in *n*-hexane at room temperature to change their surface properties to hydrophobic, then rinsed with acetone and allowed to air-dry. The bead contact angle, θ, was varied by using mixtures of DI water and different volume fractions (V_f) of ethanol. The contact angles of the silanised glass beads were measured by depositing them gently onto the air-liquid interfaces (Figure 1). Each measurement was repeated on ten different beads. Tensiometry was used to measure the surface tension of the solutions.

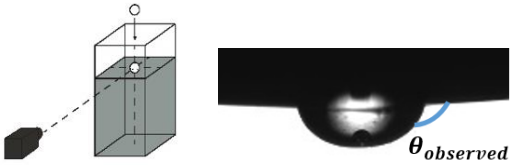

Figure 1: Contact angle analysis in a cuvette (left) and contact angle measurement of silanised bead (right)

By pouring the beads gently onto a static air-liquid interface from a paper funnel located 30 mm above the initial liquid surface, a raft was initially formed. A Basler camera (acA1929-155µm) was used to record the experiment and observed the formation of powder Island. The grains were then poured centrally at a constant flow rate of 0.12 ± 0.01 g/s. Two different cells (static and mixing vessel) were used and the dimension of both cells are summarised in Table 1. As indicated in Figure 2 (a), the wicking criterion is the detachment of grains from the interface, and the detaching criterion is the detachment of whole island from the interface. When either of these phenomena is observed, bead addition to the system is stopped, and the critical depth of island, h*, is recorded. Once an island had been created, the impellers were rotated at 3.3 rev/s, depicted in Figure 2 (b). All the measurements were repeated five times under the same conditions, and error bars indicate the standard deviation of the measured values.

Table 1: Dimensions, surface area ratio and aspect ratio of static cell and mixing vessel

Cell	Height (cm)	Length (cm)	Width (cm)	Surface area ratio	Aspect ratio (length/width)
Static	15.5	11.0	8.0	1	1.38
Mixing vessel	15.0	10.3	2.2	0.55	4.68

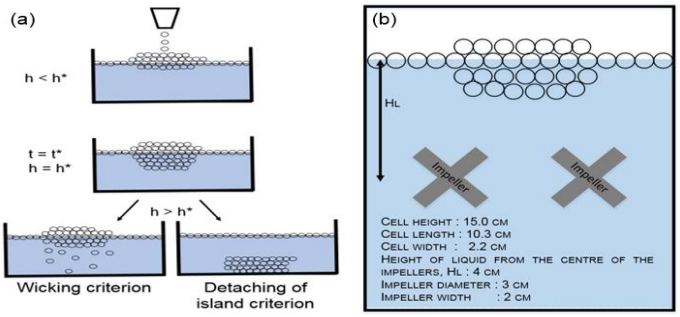

Figure 1: Experimental setup to investigate the islands formed at static air-liquid interface. Wicking and island detachment were alternatively observed with beads having contact angle θ > θ (a). Experimental setup to investigate islands formed at air-liquid interface with a moving fluid (b).*

3. Results

3.1 Contact Angle

It can be seen from the data obtained from contact angle and surface tension measurements that as V_f increases, surface tension decreases, which leads to decreasing contact angle. The surface tensions of the

ethanol solutions were consistent with those reported in the literature (Khattab et al. 2012), leading to a range of contact angles, varying from 98 ± 1.5˚ to 57 ± 3.9˚ as V_f increases from 0 to 0.5.

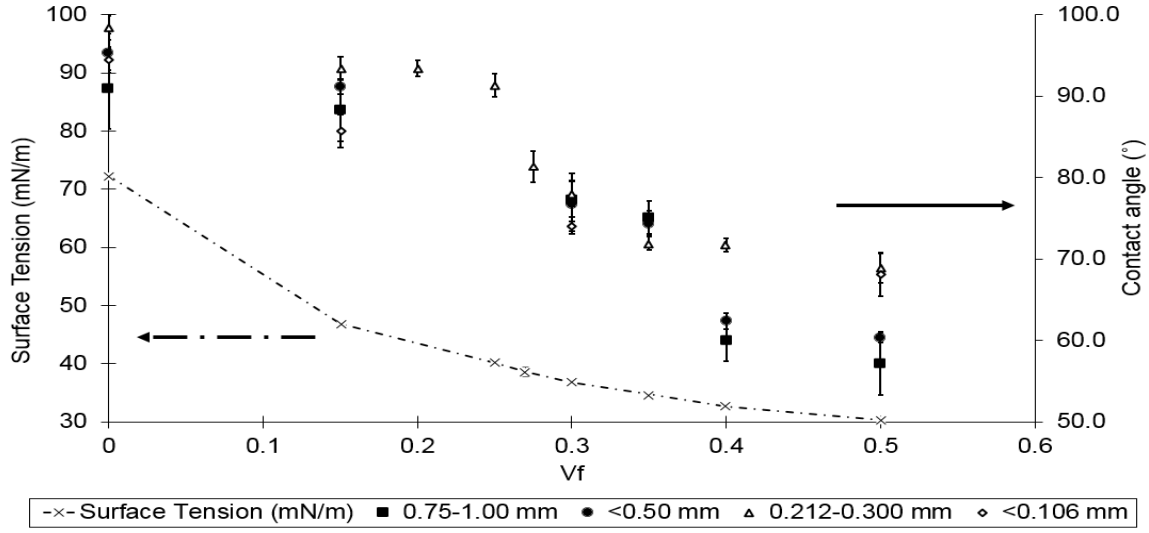

Figure 3: Contact angle of silanised glass beads of different diameter, d_p as a function of the liquid ethanol volume fraction, V_f. The crosses refer to the surface tension as a function of V_f.

3.2 Forced Impregnation with Varying Island Thickness

Figure 4 (left) shows pictures of the islands taken just before the onset of wicking or detaching and were used to measure h* above which the liquid wicks in the pores of these islands. Smaller beads show a higher critical island depth. The critical island depths as a function of contact angle are given in Figure 4 (right). Islands' depth lower than the critical depth were stable while islands' depth higher than critical depth experienced either wicking or detachment. As V_f in the system increased, the contact angle decreased which resulted in a strong decrease of the critical depth of island. Hence, h* is found to be dependent on the bead size and contact angle.

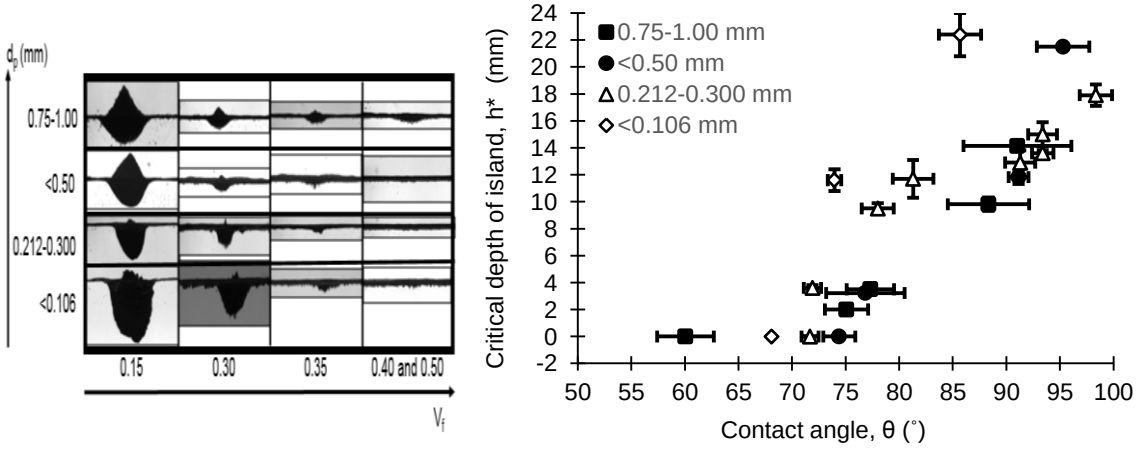

Figure 4: Critical island depth, h^*, formed by silanised glass beads of different d_p at different V_f (left). Effect of the bead contact angle and particle size on the critical island depth, h (right).*

As discussed by Raux et al. (2013), hydrostatic pressure, $P = \rho g h^*$, plays a role in changing the shape of the air-liquid interface in the pores between the beads at the bottom of the island. The Laplace pressure compensates for the hydrostatic pressure of liquid, inducing a curvature, $C = \rho g h^*/\gamma$ and this promotes the wicking process. Figure 4 (right) shows that h* increases reasonably linearly with θ, in qualitative agreement with the theory developed by Raux et al. (2013) as h* formed with beads having contact angle $\theta > \theta_0$* (critical contact angle for wicking with a flat meniscus). However, this theory is derived under the assumption of

uniform interfacial curvatures and it does not consider the situations where the contact lines have significant undulations (Cooray et al. 2017) and the contact angle may vary significantly with the increased curvature (Şenbil et al. 2015). In contrast to Raux et al. (2013), our experiments are performed by pouring the grains at a constant flow rate and this results in the critical island depth increasing significantly with decreasing grain size, as shown in Figure 4 (right).

Wicking is not always observed when pouring grains at the interface; as illustrated in Figure 5, the detachment of the whole island can also occur, leading to the formation of a lump that is wet outside and dry inside. Wicking is observed at the bottom of the island constructed from larger beads, d_p (mm) = 0.75-1.00 and <0.50 when θ is in the range between 60˚ and 95˚, as shown in Figure 5 (a)-(c), or from smaller beads, d_p (mm) = 0.212-0.300 and <0.106 when θ is in the range between 68˚ and 72˚. The whole island detached from the interface for smaller beads, d_p (mm) = 0.212-0.300 and <0.106 when θ is higher than 74˚, as shown in Figure 5 (d)-(f). Figure 5 (g) and (h) shows that when $V_f \geq 0.40$, which corresponds to θ < 77˚, the system is unable to support islands for bead sizes ranging from <0.106 to 1.00 mm, resulting in the glass beads piercing through the interface and sinking. It is interesting to observe a jet of grains encountered the liquid and crossed the interface that only happened among the smaller beads, Figure 5 (h). Lagubeau (2010) showed that the shape of jet depends strongly on the height where the nozzle from (a position where the jet originates). A state diagram is plotted in Figure 6, which reflects the effect of grain size on the critical depth of the island formed, that of "wicking" or "detaching" (grey part).

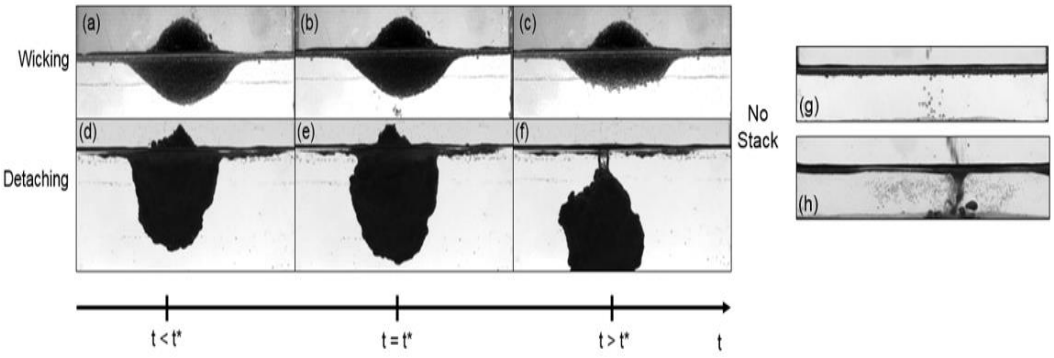

Figure 5: Images of islands at V_f=0.15, (a)-(c) experienced wicking (for d_p =0.75-1.00 mm), (d)-(f) experienced detaching from the interface (for d_p = 0.212-0.300 mm). Images of the system that can only support rafts instead of islands at Vf ≥ 0.40. d_p = 0.75 – 1.00 mm (g) and d_p =0.212-0.300 mm (h).

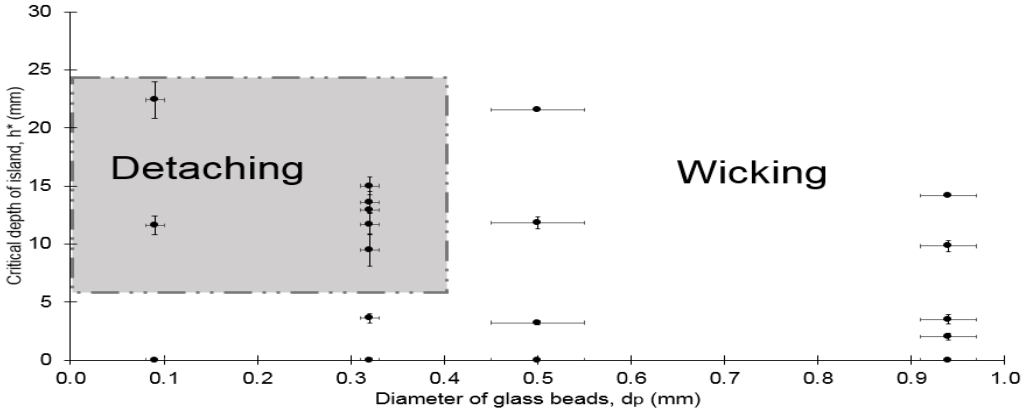

Figure 6: State diagram that separates "wicking" and "detaching" of islands.

3.3 Flow Field

The experiments in the mixing vessel were carried out using two different directions of the rotation at V_f=0.15, Figure 7 (i) and (ii). Waves were initially generated at the interface, which caused the deformation of the interface and the erosion of island. The larger bead fractions, d_p (mm) = 0.75-1.00 and <0.50, were experiencing wicking when the agitation was started. The shape of the bottom of the island changed from

spherical to flat due to the wicking induced by the liquid flow. Then the whole island detaches from the interface as a lump. As described in the previous paragraph, the island built by smaller bead fractions, d_p (mm) = 0.212-0.300 and <0.106 were always found to experience detaching from the interface in the static cell, without any agitation when θ is in the range between 74˚ and 98˚. It was decided to study how shallow islands with h < h* behave during agitation. It is interesting to observe the island composed of small beads, both sides of the raft progressively diminished toward the island during the agitation. The liquid flow destabilised the raft and island, which both fall into the liquid. On the contrary, with larger beads, the liquid flow is not sufficient to entrain the raft into the liquid, as illustrated in Figure 7 (d) and (h).

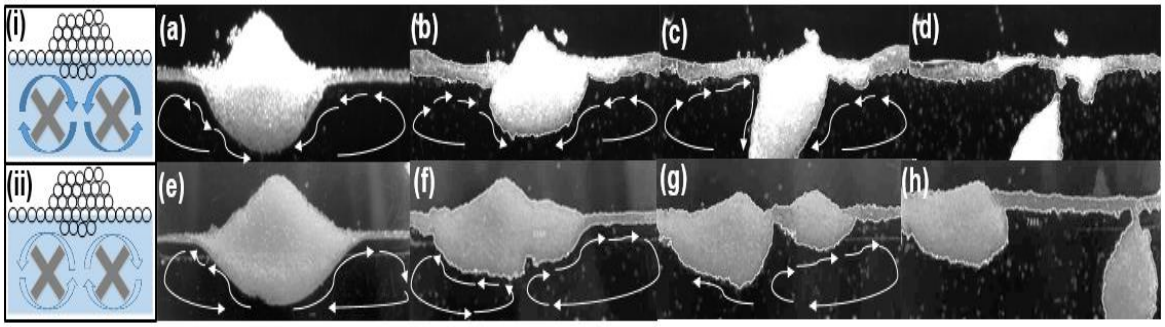

Figure 7: Direction of the impellers rotating (i) centre-down and (ii) centre-up. Images of two different islands detached from the interface. From (a) to (d) island experienced centre-down rotation and from (e) to (h) island experienced centre-up rotation (V_f=0.15, d_p=0.75-1.00 mm)

The detachment time of island from the interface that built by four different sizes of glass beads are summarised in Table 2 and the time required to detach islands built by smaller bead fractions is relatively shorter than larger beads fractions. It is found that the time required to detach the island in centre-up rotation is much longer (30-50%) than centre-down rotation. In the centre-up configuration, the flow promotes much more wicking and erosion of island than the centre-down rotation. The flow shears the island apart, creates smaller islands that are less prone to sinking, delays the detachment time of island from the interface and reduces the size of lump formation. Hence, the flow field created by centre-up rotation is found to be more ideal in the dispersion process. Most zones of the mixing vessel, which are distant from the impellers are barely affected by the agitation, especially at the bottom of vessel, which explains why the whole island accumulated as a lump at the bottom of the cell during the agitation.

Table 2: Time required to detach the island from the interface by using two different directions of the impellers at V_f=0.15 (for d_p= 0.75-1.00, <0.50, 0.212-3.00 and <0.106 mm)

Direction of the impellers	d_p (mm)	Island detachment time (s)
Centre-down	0.75-1.00	53±4
Centre-down	<0.50	373±13
Centre-down	0.212-0.300	6±1
Centre-down	<0.106	5±0.5

Direction of the impellers	d_p (mm)	Island detachment time (s)
Centre-up	0.75-1.00	161±10
Centre-up	<0.50	796±11

4. Conclusions

This study shows that dispersion of powders depends on physico-chemical properties of the powder grains and the liquid flow. The critical island depth on a static liquid increases with decreasing grain radius and increasing wettability. The phenomena of wicking or island detachment depends on the particle size and contact angle. The detachment of the island from the interface is the precursor to powder lump formation, since dispersion is hindered thereafter by the entrained air, with negative consequences for the product, as well as consumer perception and preference. It was also observed that introducing flow in the liquid by agitation does not necessarily improve the dispersion process and can facilitate lump formation. More work is needed to enable assigning the optical flow in order to disperse powders with specific physico-chemical properties. Lastly, more complex grains such as food powders will be used in this study.

References

Ban S., Wolfram E., Rohrsetzer S., 1987, The condition of starting of liquid imbibition in powders. Colloids and surfaces, 22, 301–309.

Cooray H., Cicuta P., Vella D., 2017, Floating and Sinking of a Pair of Spheres at a Liquid–Fluid Interface. Langmuir, DOI:10.1021/acs.langmuir.6b03373.

Dupas J., Verneuil E., Van Landeghem M., Bresson B., Forny L., Ramaioli M., Lequeux F., Talini L., 2014, Glass Transition Accelerates the Spreading of Polar Solvents on a Soluble Polymer. Physical Review Letters, 112, 188302.

Dupas J., Forny L., Ramaioli M., 2015, Powder wettability at a static air–water interface. Journal of Colloid and Interface Science, 448, 51–56.

Dupas J., Girard V., Forny L., 2017, Reconstitution properties of sucrose and maltodextrins. Langmuir, DOI: 10.1021/acs.langmuir.6b04380.

Forny L., Marabi A., Palzer S., 2011, Wetting, disintegration and dissolution of agglomerated water soluble powders. Powder Technology, 206, 72–78.

Gurupatham S., Hossain M., Dalal B., Fischer I.S., Singh P., Joseph D.D., 2012, Breakup of particle clumps on liquid surfaces. Powder Technology, 217, 288–297.

Hamlett C.A.E., Shirtcliffe N.J., McHale G., Ahn S., Bryant R., Doerr S.H., Newton M.I., 2011, Effect of particle size on droplet infiltration into hydrophobic porous media as a model of water repellent soil. Environmental Science and Technology, 45, 9666–9670.

Khattab I.S., Bandarkar F., Fakhree M.A.A., Jouyban A., 2012. Density, viscosity, and surface tension of water+ethanol mixtures from 293 to 323K. Korean Journal of Chemical Engineering, 29, 812–817.

Lagubeau G., 2010, Interfaces à grains, et autres situations de mouillage nul (in French).

Mitchell W.R., Forny L., Althaus T.O., Niederreiter G., Palzer S., Hounslow M.J., Salman A.G., 2015, Mapping the rate-limiting regimes of food powder reconstitution in a standard mixing vessel. Powder Technology, 270, 520–527.

Özcan-Taşkin G., 2006, Effect of scale on the draw down of floating solids. Chemical Engineering Science, 61, 2871–2879.

Raux P.S., Cockenpot H., Ramaioli M., Quéré D., Clanet C., 2013, Wicking in a powder. Langmuir, 29, 3636–3644.

Şenbil N., He W., Démery V., Dinsmore A.D., 2015, Effect of interface shape on advancing and receding fluid-contact angles around spherical particles. Soft Matter, 11, 4999–5003.

Vella D., Metcalfe P., Whittaker R., 2005, Equilibrium Conditions for the Floating of Multiple Interfacial Objects.

Washburn E.W., 1921, The dynamics of capillary flow. Physical Review, 17, 273–283.